

ASU COMPACT XFEL*

W. S. Graves[†], J. P. J. Chen, P. Fromme, M. R. Holl, R. Kirian, L. E. Malin, K. E. Schmidt,
J. C. H. Spence, M. Underhill, U. Weierstall, N. A. Zatsepin, C. Zhang,
Arizona State University, Tempe, USA
P. D. Brown, K. H. Hong, D. E. Moncton, MIT, Cambridge, USA
E. A. Nanni, C. Limborg-Deprey, SLAC, Menlo Park, USA

Abstract

Arizona State University (ASU) is pursuing a concept for a compact x-ray FEL (CXFEL) that uses nanopatterning of the electron beam via electron diffraction and emittance exchange to enable fully coherent x-ray output from electron beams with an energy of a few tens of MeV. This low energy is enabled by nanobunching and use of a short pulse laser field as an undulator, resulting in an XFEL with 10 m total length and modest cost. The method of electron bunching is deterministic and flexible, rather than dependent on SASE amplification, so that the x-ray output is coherent in time and frequency. The phase of the x-ray pulse can be controlled and manipulated so that new opportunities for ultrafast x-ray science are enabled using attosecond pulses, very narrow line widths, or extremely precise timing among multiple pulses with different colors. These properties may be transferred to large XFELs through seeding with the CXFEL beam. Construction of the CXFEL accelerator and laboratory are underway, along with initial experiments to demonstrate nanopatterning via electron diffraction. An overview of the methods and project are presented.

INTRODUCTION

ASU has embarked on a multiphase effort to develop powerful compact x-ray sources, beginning with the compact x-ray light source [1] (CXLS) that is now under construction and will be operational by end of 2017. CXLS uses an x-band photoinjector, standing wave linac, and high power lasers to produce x-rays via inverse Compton scattering (ICS) with projected flux of about 10^8 photons per shot at the high repetition rate of 1 kHz. The 35 MeV linac is expected to produce photon energies in the range 1-35 keV with pulse length of 100 fs to 1 ps. CXFEL is the planned second phase of development and is closely based on CXLS equipment. CXFEL will transform the incoherent ICS emission of CXLS into a fully coherent x-ray laser by creating ‘nanobunches’ using a combination of methods including diffraction of the electron beam from a patterned silicon crystal [2–5] at energy of 4-10 MeV and transformation of the resulting spatial pattern, or density modulation, into the longitudinal dimension using emittance exchange (EEX) [6]. CXLS is designed to be easily upgraded to CXFEL by reconfiguring the bunch compression chicane into a double dogleg EEX

line. All of the electron optics and equipment needed to pattern the electron beam, with the exception of the EEX line, are included in the phase 1 CXLS, enabling preliminary experiments to study and understand the generation and manipulation of patterned electron beams.

TECHNICAL DESCRIPTION

The CXFEL components are shown in Figure 1. Beginning at the right end of the figure is the 4.5 cell x-band photoinjector [7] that accelerates the beam to 4 MeV. Following ports for the cathode laser is the first of three short 35 cm long linac sections, each of which is an innovative 20-cell standing-wave linac [8] adapted to our 9.3 GHz RF frequency. SLAC spinoff company Tibaray LLC is producing the photoinjector and linac. The first linac section L1 can accelerate the beam up to 12 MeV and/or adjust the time-energy chirp for optimum diffraction in the thin silicon crystal that sits just downstream of it. After the crystal the two linac sections L2 and L3 are jointly powered and phased to accelerate the beam to a maximum of 35 MeV. The photoinjector and linac L1 are powered by one RF transmitter with high power waveguide attenuator and phase shifter to arbitrarily split RF amplitude and phase among the two devices. A second RF transmitter powers L2 and L3 as well as the deflector cavity in the downstream EEX line. The RF transmitters are Scandinova solid-state K1A modulators driving L3 L6145-01 9.3 GHz klystrons capable of 6 MW output power in 1 microsecond pulses at repetition rates up to 1 kHz. The transmitters are now in final testing at the vendor and have demonstrated better than 100 ppm RMS voltage stability.

Following L3 is a set of 4 quadrupoles (Q1-Q4) arranged as a variable demagnification telescope to image the electron beam at the crystal plane to a downstream point. For electron microscopy studies the beam is spatially imaged onto a profile monitor PRO6 in the EEX line. The imaging requirement is different to generate nanobunches at the output of the EEX line. In this case the spatial image of the silicon grating is never formed, but rather a matching condition with tilted ellipses [2] is generated at the entrance to the EEX line so that the original modulation created by the crystal is transferred to the longitudinal dimension at the EEX output. The EEX line consists of the 4 bend magnets B1-B4, an RF deflector cavity and accelerator cavity that are independently phased and powered, along with sextupoles S1-S3 and octopole O1 for aberration correction. Following the EEX line is a quadrupole triplet (Q5-Q7) that focuses

* This work was supported by NSF Accelerator Science award 1632780, NSF BioXFEL STC award 1231306, DOE contract DE-AC02-76SF00515, and ASU.

[†] wsg@asu.edu

Content from this work may be used under the terms of the CC BY 3.0 licence (© 2018). Any distribution of this work must maintain attribution to the author(s), title of the work, publisher, and DOI.

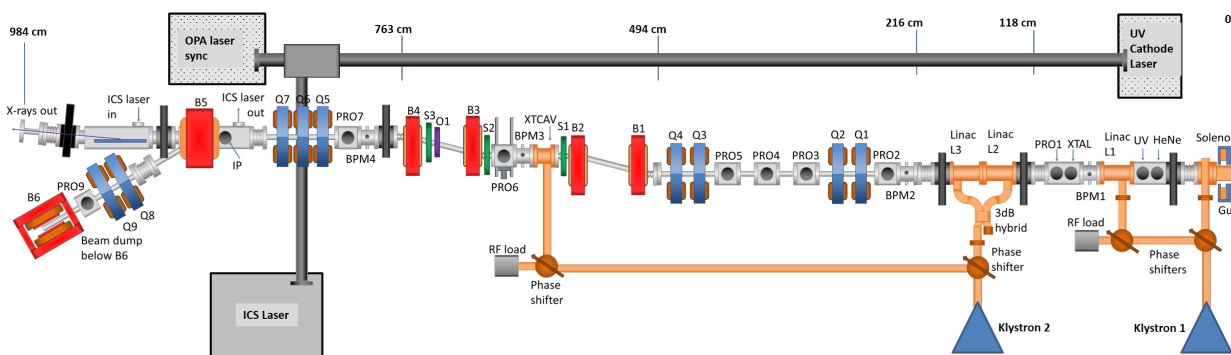


Figure 1: Major components of CXFEL. The photoinjector is at the right end. A short linac (L1) modifies the electron beam energy and chirp before diffraction into a nanopattern. The beam is further accelerated in linacs L1 and L2, then a telescope demagnifies the pattern and matches to the emittance exchange line before the laser interaction point. The entire assembly is 10 m long.

the electron beam to micron size at the ICS interaction point (IP) where the patterned electron bunches radiate coherently in the ICS laser field. Downstream of the IP the beam is deflected 30 degrees horizontally (B5) and then 90 degrees vertically (B6) into a beam dump. Nominal charge per pulse is 1 pC so that the average power into the dump is <1 W.

The photocathode laser is a Lightconversion Pharos Yb:KGW amplifier with integral UV conversion generating up to 1.5 mJ at 1030 nm, and 150 μJ at 4th harmonic 258 nm, in 180 fs pulses. The Pharos also contains the laser oscillator running at 72.6 MHz, the 128th subharmonic of the 9300 MHz RF frequency. The Pharos is located in local shielding adjacent to the photoinjector to present a short beam path to the cathode and to facilitate synchronization with the electron beam and ICS laser. The ICS laser is a Trumpf Dira 200-1 Yb:YAG amplifier generating 200 mJ in 1.5 ps pulses. Both lasers operate at 1 kHz to match the accelerator repetition rate. The Dira is located in a laser room adjacent to the ICS interaction point.

Timing synchronization of the electron beam, lasers, and x-rays is a critical performance parameter for linac-based light sources. Our initial goal is sub-100 fs timing synchronization of the beams, and eventually sub-10 fs synchronization. The low-level RF (LLRF) and laser oscillator are locked to a Wenzel MXO RF master oscillator with -176 dBc/Hz intrinsic phase noise. The laser oscillator uses a Menlo Systems custom SYNCHRO RRE with fast and slow piezo loops to lock to the MO and control the Pharos timing. The Dira ICS laser is synchronized to the Pharos by splitting a small portion of the Pharos output to white light generation for seeding an optical parametric chirped pulse amplifier (OPCPA) that measures and corrects the Dira timing. This method has demonstrated sub-10 fs timing [9]. The LLRF that drives the RF transmitters is being adapted from the LCLS upgrade in collaboration with SLAC, and has demonstrated RMS phase jitter <0.01 RF degrees [10] (3 fs at 9300 MHz). The compact size of the facility and high degree of care taken with the laboratory construction are expected to contribute to ultrastable timing.

In addition to timing stability, the source demands stability in pointing, energy, and flux, which in turn depend on stability of all power supplies and the laboratory environment. All magnet power supplies have stability in current ripple and drift of <100 ppm, and the solid-state RF modulators have demonstrated the best possible stability. Initial tests of the Dira laser indicate pointing stability less than 5 μrad and power stability of 0.3% over 12 hour long term tests.

LABORATORY FACILITIES

ASU is constructing a new Biodesign C building that contains 25,000 sq.ft. of laboratory space on the basement level to house CXLS and CXFEL (Figure 2). There are two mirror-image laboratories to house independent light sources. The phase 1 construction will finish the CXLS lab. The labs are highly customized to provide the optimum environment needed for stable operation. The slab floor is 6 ft thick and is mechanically isolated from the surrounding building to avoid vibration. The labs are rated at vibration criterion VC-E, equivalent to state-of-the-art electron microscopy labs. The accelerator vaults and x-ray hutches are ISO class 8 cleanrooms with non-turbulent airflow. The laser labs are ISO class 7 cleanrooms. During construction the iron rebar that was used in the accelerator areas was hand-selected for low magnetic field, and degaussed where needed. Background fields were repeatedly measured with the result that the ambient magnetic field in the labs is at Earth's background. The RF room containing the RF transmitters is a sealed aluminum Faraday cage with special penetrations for waveguide and other signals in order to isolate electromagnetic noise emitted by the pulsed transmitters. Air temperature control is ±0.5°C in the vault, RF room, and x-ray hutch, and ±0.25°C with relative humidity 35-40% in the laser room. All equipment racks are actively cooled. The relatively small space and equipment needs of CXFEL makes this precise environmental control practical and cost effective.

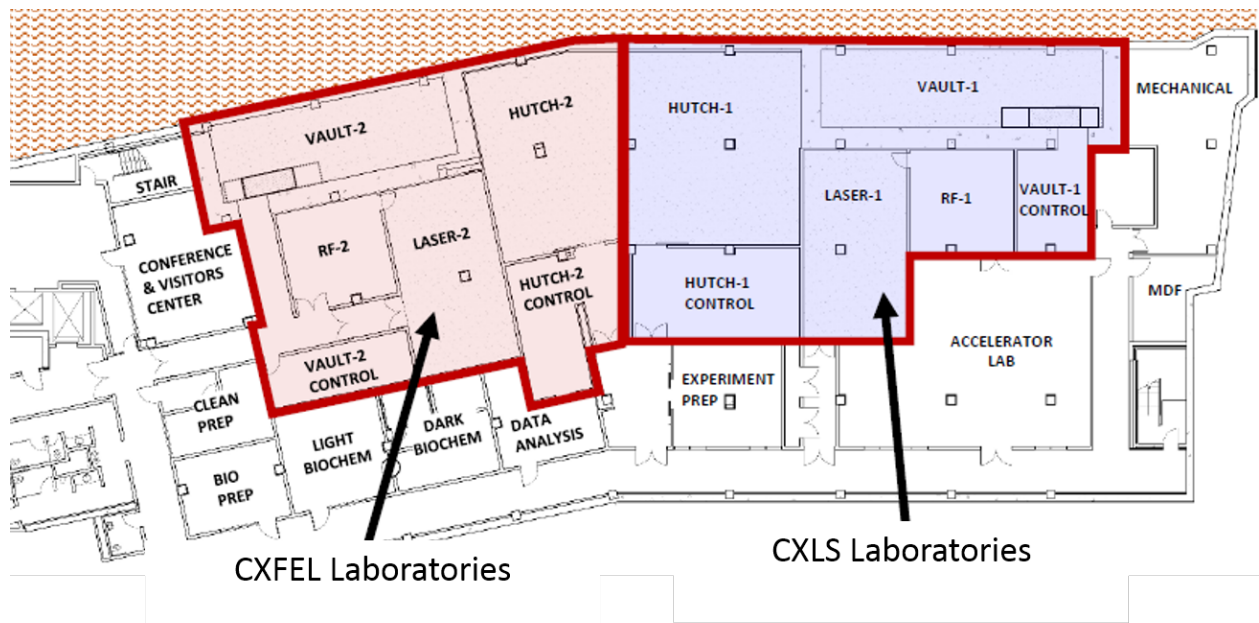


Figure 2: ASU laboratories under construction in new Biodesign C building to house CXLS and CXFEL. Vault, laser room, and x-ray hutch are on slabs isolated from surrounding building meeting VC-E vibration criteria.

ESTIMATED PERFORMANCE

CXFEL will have fully coherent output, unlike the large XFELs that lack temporal coherence, with properties that can be manipulated in novel ways. Frequency chirps can be reproducibly programmed and x-ray optics used to compress the few fs long pulses to below 1 fs. The method allows for coherent control of the phase, frequency, bandwidth, pulse length and amplitude of the x-ray pulses, and enables a variety of 2-color or multi-color experiments with precisely tunable femtosecond delays for pump-probe experiments, and perhaps even sub-cycle phase-locking of the multiple colors. The CXFEL can transfer many of these properties to beams at large XFELs by providing a coherent seed with power orders of magnitude above the SASE startup noise.

The electron beam must meet criteria in emittance, energy spread, and peak current. In order for good coupling of electron emission into the fundamental x-ray mode the emittance ϵ_n should satisfy $\frac{\epsilon_x}{\gamma} \leq \frac{\lambda_x \beta_x}{4\pi L_G}$ (eq. 73 of [11]) where $\beta_x \approx 1$ mm is the accelerator lattice beta function at the interaction point. This is an example where the extremely short gain length $L_G < 100 \mu\text{m}$ enabled by using a laser undulator is advantageous because the ratio $\beta_x/L_G \approx 20$ in the emittance equation rather than unity for a conventional FEL enables CXFEL to meet the emittance requirement. Taking example beam parameters for 8 keV photons where $\lambda_x = 0.155$ nm, and electron energy of 22 MeV ($\gamma = 45$) the emittance requirement becomes $\epsilon_n \leq 11$ nm. While this is a very low emittance, it can be achieved at low charge of 1 pC by reducing the cathode spot size. The emittance varies linearly with spot size so that a laser spot with RMS radius $20 \mu\text{m}$ ($80 \mu\text{m}$ diameter) will produce an initial emittance of 10 nm. Simulations [2] show that 10 nm emittance can

be maintained through the 8 m of transport from cathode to interaction point. These simulations show that the peak current is 3 A at the gun exit for a 300 fs bunch length.

One result of the nanopatterning method is that the transverse emittance upstream of the EEX line determines the energy spread and current at the IP downstream. The relative energy spread $\delta = \frac{\Delta y}{y}$ must be lower than the FEL parameter $\rho_{\text{FEL}} \approx 5 \times 10^{-4}$, and the peak current should be as high as possible. Because EEX results in an exact swap of transverse and longitudinal emittances we can predict that downstream of EEX, $\delta \times c\tau = \epsilon_n/\gamma$. Our nominal design is for 10,000 periods of 0.155 nm x-rays, thus the bunch length at the IP is $c\tau = 1.55 \mu\text{m}$ or 5 fs. For 1 pC of charge this results in 200 A peak current, and, conserving emittance, $\delta = 1.5 \times 10^{-4} < \rho_{\text{FEL}}$. We note that the longitudinal emittance upstream of the EEX must be equal to or better than the transverse emittance 10 nm, which simulations show is satisfied at the low charge and current generated by the photoinjector. Summarizing this section, the electron beam parameters at the interaction point are $\epsilon_n = 10$ nm, $\delta = 1.5 \times 10^{-4}$, peak current = 200 A, bunch length = 5 fs, $Q = 1$ pC, lattice parameter $\beta_x = 1$ mm to produce rms beam size of 0.3 microns. Using these parameters we find that indeed $\rho_{\text{FEL}} = 4.7 \times 10^{-4}$ for 8 keV photons, similar to large XFELs, and a surprising result for such a modest charge, energy, and current. The gain length for 8 keV photons produced by a 22 MeV beam is just $72 \mu\text{m}$. An electron beam with this set of parameters is very well matched to the coherent x-ray mode. We predict the CXFEL output properties from this beam will be a peak power of 2 MW with transform-limited bandwidth of 0.01% and pulse length 5 fs that can be chirped to 0.1% bandwidth and then compressed with multilayer optics to 0.5 fs.

ACKNOWLEDGMENT

We thank Vinod Bharadwaj, Sergio Carbajo, Mitch D'Ewart, Valery Dolgashev, Joe Frisch, Ernie Ihloff, Arvinder Sandhu, Sami Tantawi, and Andrew Young for many helpful technical discussions. This work was supported by NSF Accelerator Science award 1632780, NSF BioXFEL STC award 1231306, DOE contract DE-AC02-76SF00515, and ASU.

REFERENCES

- [1] W. S. Graves *et al.*, “Compact x-ray source based on burst-mode inverse Compton scattering at 100 kHz,” *Phys. Rev. ST Accel. Beams*, vol. 17, p. 120701, Dec 2014.
- [2] E. A. Nanni, W. S. Graves, and D. E. Moncton, “Nano-modulated electron beams via electron diffraction and emittance exchange for coherent x-ray generation,” arXiv:1506.07053, 2015.
- [3] E. Nanni *et al.*, “Measurements of transmitted electron beam extinction through Si crystal membranes,” in *Proc. of Int. Particle Accel. Conf (IPAC2016)*, no. 7 in International Particle Accelerator Conference, (Busan, Korea), pp. 1611–1614, May 2016.
- [4] L. Malin *et al.*, “Comparison of theory, simulation, and experiment for dynamical extinction of relativistic electron beams,” in *Proc. of Int. Particle Accel. Conf (IPAC2017)*, (Copenhagen, Denmark), p. THPAB088, May 2017.
- [5] C. Zhang *et al.*, “Experiments in electron beam nanopatterning,” in *Proc. of 2017 Int'l Free Electron Laser Conference (FEL2017)*, (Santa Fe, USA), p. TUP038, August 2017.
- [6] E. A. Nanni and W. S. Graves, “Aberration corrected emittance exchange,” *Phys. Rev. ST Accel. Beams*, vol. 18, p. 084401, Aug 2015.
- [7] W. S. Graves *et al.*, “Design of an x-band photoinjector operating at 1 kHz,” in *Proc. of Int. Particle Accel. Conf (IPAC2017)*, (Copenhagen, Denmark), p. TUPAB139, May 2017.
- [8] M. H. Nasr, Z. Li, C. Limborg, S. Tantawi, and P. Borchard, “High power tests of a novel distributed coupling linac,” in *Proc. of Int. Particle Accel. Conf (IPAC2017)*, (Copenhagen, Denmark), p. TUPAB131, May 2017.
- [9] S. Prinz, M. Häfner, M. Schultze, C. Y. Teisset, R. Bessing, K. Michel, R. Kienberger, and T. Metzger, “Active pumpseed-pulse synchronization for OPCPA with sub-2-fs residual timing jitter,” *Opt. Express*, vol. 22, pp. 31050–31056, Dec 2014.
- [10] M. D'Ewart *et al.*, “Performance of ATCA LLRF system at ICLS,” in *Proc. of Int. Particle Accel. Conf (IPAC2017)*, (Copenhagen, Denmark), p. THPVA152, May 2017.
- [11] Z. Huang and K.-J. Kim, “Review of x-ray free-electron laser theory,” *Phys. Rev. ST Accel. Beams*, vol. 10, p. 034801, Mar 2007.